The Astrophysical Journal, 685: L113–L116, 2008 October 1

SPITZER/MIPS 24 μm OBSERVATIONS OF GALAXY CLUSTERS: AN INCREASING FRACTION OF OBSCURED STAR-FORMING MEMBERS FROM $z = 0.02$ TO $z = 0.83$

Amélie Saintonge,[1] Kim-Vy H. Tran,[1] and Bradford P. Holden[2]

Received 2008 June 6; accepted 2008 August 20; published 2008 September 9

ABSTRACT

We study the mid-infrared properties of 1315 spectroscopically confirmed members in eight massive ($M_{\rm vir} \gtrsim 5 \times 10^{14}\ M_\odot$) galaxy clusters covering the redshift range from 0.02 to 0.83. The selected clusters all have deep *Spitzer*/MIPS 24 μm observations, *Hubble* and ground-based photometry, and extensive redshift catalogs. We observe for the first time an increase in the fraction of cluster galaxies with mid-infrared star formation rates higher than $5\ M_\odot\ {\rm yr}^{-1}$ from 3% at $z = 0.02$ to 13% at $z = 0.83$ ($R_P \leq 1$ Mpc). This increase is reproduced even when considering only the most massive members ($M_* \geq 4 \times 10^{10}\ M_\odot$). The 24 μm observations reveal stronger evolution in the fraction of blue/star-forming cluster galaxies than in color-selected samples: the number of dusty, strongly star-forming cluster galaxies increases with redshift, and combining these with the optically defined Butcher-Oemler members [$\Delta(B - V) < -0.2$] doubles the total fraction of blue/star-forming galaxies in the inner Mpc of the clusters to ~23% at $z = 0.83$. These results, the first of our *Spitzer*/MIPS Infrared Cluster Survey (SMIRCS), support earlier studies indicating that the increase in star-forming members is driven by cluster assembly and galaxy infall, as is expected in the framework of hierarchical formation.

Subject headings: galaxies: clusters: general — galaxies: evolution — galaxies: fundamental parameters

Online material: color figure

1. INTRODUCTION

Butcher & Oemler (1978, 1984) observed that galaxy clusters at intermediate redshift have a higher fraction of members with blue optical colors than clusters in the local universe, thus providing a key piece of evidence supporting galaxy evolution. This increase in blue members with redshift, named the Butcher-Oemler (BO) effect, was intensely debated for 2 decades (e.g., Mathieu & Spinrad 1981; Dressler & Gunn 1982). However, multiple optical studies based on spectroscopic observations have since confirmed the increase in blue, star-forming galaxies in higher redshift clusters (e.g., Couch & Sharples 1987; Caldwell & Rose 1997; Fisher et al. 1998; Ellingson et al. 2001) and found that BO galaxies reveal signs of recent and ongoing star formation. The paramount question now is have we seen only the tip of the iceberg?

Most studies of star-forming galaxies in clusters rely on rest-frame ultraviolet or optical tracers (e.g., Balogh et al. 1998; Poggianti et al. 2006), but UV/optical tracers can suffer severely from dust obscuration, especially when star formation (SF) is concentrated in the nuclear regions (Kennicutt 1998). For example, ultraluminous infrared galaxies have SF rates of $\gtrsim 1000\ M_\odot$, yet many ULIRGs fail to even be detected at UV and optical wavelengths (e.g., Houck et al. 2005). Although corrections for dust attenuation are possible, reliable estimates of SF rates cannot be achieved solely using rest-frame UV/optical observations (Bell 2002; Cardiel et al. 2003).

A substantially more robust method of determining total SF rates is with mid-infrared (MIR) imaging. The first MIR imaging of galaxy clusters at intermediate redshifts was taken with *ISO*'s ISOCAM camera, and Duc et al. (2002) found that at least 90% of the star formation was hidden at optical wavelengths. The first handful of galaxy clusters observed with the MIPS camera on the *Spitzer Space Telescope* (*SST*) have also revealed strong dust-obscured star formation (Geach et al. 2006; Marcillac et al. 2007; Bai et al. 2007).

It remains unclear as to what causes the increase in star-forming galaxy cluster members. Detailed morphological studies of blue galaxies [defined as having $\Delta(B - V) < -0.2$][3] with the *Hubble Space Telescope* (*HST*) find that most are disk systems similar to those in local clusters (e.g., Dressler et al. 1994; Couch et al. 1994); past studies also find that many show signs of interactions or mergers (Lavery & Henry 1988; Lavery et al. 1992; Couch et al. 1994; Oemler et al. 1997). More recently, studies indicate that galaxy infall is a viable explanation for the significant numbers of blue galaxies and their disturbed morphologies in intermediate-redshift clusters (e.g., van Dokkum et al. 1998b; Ellingson et al. 2001; Tran et al. 2005), a scenario supported by hierarchical clustering models (Kauffmann 1995). In this case, galaxy clusters that are accreting a significant number of new members should have a higher fraction of star-forming galaxies, especially at higher redshifts when the amount of activity was enhanced also in the field.

Here we present the first comprehensive study of *SST*/MIPS 24 μm imaging of galaxies that are spectroscopically confirmed members of eight massive ($M_{\rm vir} \gtrsim 5 \times 10^{14}\ M_\odot$) X-ray–luminous clusters spanning a wide redshift range ($0.02 < z < 0.83$). After presenting the data in § 2, we focus our analysis in § 3 and § 4 on the evolution of star-forming members with redshift. A cosmology with (H_0, Ω_M, Ω_Λ) = (70 km s^{-1}, 0.3, 0.7) is assumed throughout the Letter; at $z = 0.83$, the look-back time is ~7 Gyr.

2. DATA

We have assembled a data set of eight galaxy clusters at $0.02 \leq z \leq 0.83$ that have a total of 1315 spectroscopically confirmed members. The core of our sample is composed of five clusters spanning the entire redshift range with large spectroscopic membership, uniform multifilter optical photometry, and deep *SST*/MIPS imaging.[4] For the part of the analysis that does

[1] Institute for Theoretical Physics, University of Zurich, CH-8057 Zurich, Switzerland.

[2] UCO/Lick Observatories, University of California, Santa Cruz, CA 95064.

[3] $\Delta(B - V)$ is the color offset from the red sequence fit to the cluster ellipticals.

[4] This work is based on observations made with the *Spitzer Space Telescope,* which is operated by the Jet Propulsion Laboratory, California Institute of Technology, under a contract with NASA.

TABLE 1
PROPERTIES OF SELECTED CLUSTERS

Name	Coordinates (R.A., Decl.) (J2000.0)	z Range[a]	L_X[b] (10^{44} ergs s^{-1})	N_z[c]	N_s[d]	N_{24}[e]	t_{int} (s pixel^{-1})	F_{bg} (MJy sr^{-1})	$F_{50\%}$ ($M_\odot$ yr^{-1})
Coma	12 59 35.7, +27 57 34	0.013−0.033	9.0 ± 0.2	244	63	134 (2)	73	32.8	0.02
A1689	13 11 29.5, −01 20 17	0.17–0.22	21.4 ± 1.0	81	52	12 (2)	…[f]	…	1.4[f]
MS 1358+62	13 59 50.4, +62 31 03	0.315–0.342	10.2 ± 0.7	171	73	21 (3)	2700[g]	20.6	0.75
CL 0024+17	00 26 35.7, +17 09 43	0.373–0.402	2.9 ± 0.1	205	51	11 (6)	2700[g]	48.5	1.48
MS 0451−03	04 54 10.9, −03 01 07	0.52–0.56	21.0 ± 0.4	242	38	8 (5)	2700[g]	35.0	3.34
MS 2053−04	20 56 21.3, −04 37 51	0.57–0.60	6.5 ± 0.4	85	43	15 (8)	1950	35.2	5.04
MS 1054−03	10 57 00.0, −03 37 36	0.80–0.86	16.4 ± 0.8	142	75	13 (8)	3600[g]	47.4	4.54
RX J0152−13	01 52 43.9, −13 57 19	0.81–0.87	18.6 ± 1.9	147	61	19 (8)	3600[g]	31.9	3.05

NOTE.—Units of right ascension are hours, minutes, and seconds, and units of declination are degrees, arcminutes, and arcseconds.
[a] Cluster members selected within this redshift range, as in H07 (Coma, MS 1358, MS 2053, MS 1054, RX J0152), Duc et al. 2002 (A1689), and Moran et al. 2007 (CL 0024 and MS 0451).
[b] Bolometric X-ray luminosities from H07 (Coma, MS 1358, MS 2053, MS 1054, RX J0152), Bardeau et al. 2007 (A1689), Donahue et al. 1999 (MS 0451), and Zhang et al. 2005 (CL 0024).
[c] Total number of spectroscopically confirmed members (magnitude-limited selection). Redshifts are taken from Beijersbergen 2003, Duc et al. 2002, Fisher et al. 1998, Moran et al. 2005, Moran et al. 2007, Tran et al. 2005, Tran et al. 2007, and Demarco et al. 2005, respectively.
[d] Number of confirmed members within 1 Mpc of the cluster center and brighter than $M_B = -19.5 + 5 \log h$.
[e] Number of MIPS detections in the cluster; values in parentheses are the number of galaxies within N_s with SF rates $\geq 5\ M_\odot$ yr^{-1}.
[f] We are using ISOCAM mid-IR data from Duc et al. 2002 for A1689.
[g] Over the central 5′ × 5′of the MIPS image.

not depend on rest-frame $(B - V)$ color, we fold into the sample three additional clusters: A1689 for which MIR data from ISOCAM is available (Duc et al. 2002), and CL 0024 and MS 0451, both of which have extensive redshift catalogs (Moran et al. 2005) and MIPS observations. Observational details for all clusters are in Table 1.

2.1. *Optical Photometry and Spectroscopy*

The optical photometry for the five main clusters is from Holden et al. (2007, hereafter H07), where magnitudes and colors were derived from Sersic models fitted to *HST*/WFPC2 images (MS 1358, MS 2053, and RX J0152), *HST*/ACS images (MS 1054), and SDSS mosaics for Coma. The conversion to rest-frame values is done by interpolating between the passbands (Blakeslee et al. 2006) and has errors of ∼0.02 mag. The mass-to-light ratios (M/L_B) and stellar masses were calculated using the relation between rest-frame $(B - V)$ color and M/L_B; see H07 for details and a discussion on the associated errors.

2.2. *MIPS* 24 μm *Imaging*

All MIPS data sets were retrieved from the *Spitzer* public archive. Individual frames were corrected with scan mirror position-dependent flats and then mosaicked with the MOPEX software (Makovoz & Khan 2005) to a pixel size of 1.2″.[5] Integration times (t_{int}) and background levels (F_{bg}) in these mosaics are given in Table 1. Photometry was performed with APEX (Makovoz & Marleau 2005) using a 3″ diameter aperture and an aperture correction of 9.49 as given in the MIPS data handbook. A small aperture is necessary to avoid contamination in the deep and crowded cluster fields. The fluxes are consistent with results from PSF-fitting photometry with scatter from a 1 : 1 relation in the range of 15–25 μJy.

To estimate the completeness of each MIPS catalog, we added to the mosaics artificial sources modeled on the PSF. To avoid overcrowding, we simulated 30 signals at once and repeated the process 30 times for each cluster (the 50% completeness limits, $F_{50\%}$, are presented in Table 1). Finally, the MIPS sources were matched with the optical catalogs using a 2″ search radius (Bai et al. 2007). From randomization of the MIPS coordinates, we estimate the rate of false identification to be 7% ± 4%, and little dependency of this error rate on redshift or color is observed.

[5] The instrumental pixels are 2.55″ in size, but the finer sampling helps in improving the characterization of the PSF.

2.2.1. *Star Formation Rates*

Star formation rates are based on the 24 μm fluxes. First, the total infrared luminosity ($F_{8-1000\,\mu m}$) of each galaxy was determined using a family of infrared spectral energy distributions (SEDs) from Dale & Helou (2002). We choose the range of SEDs that are representative of the galaxies in the Spitzer Infrared Nearby Galaxies Survey (Dale et al. 2007) and at each redshift adopt the median conversion factor from $F_{24\,\mu m}$ to $F_{8-1000\,\mu m}$ given by these models. At $0.4 \lesssim z \lesssim 0.6$, the error due to the adopted conversion factor is ∼20%, but the error increases to a factor of 1.5–2.0 at lower and higher redshifts. For the parts of our analysis that are sensitive to the SF rates, we take these errors into account. As a check, we note that our total infrared luminosities in MS 1054 agree well with the values in Bai et al. (2007). The conversion from total infrared luminosities to star formation rates is done following Kennicutt (1998).

We assume that the emission at 24 μm is due to star formation, but it could also be due to dust-enshrouded active galactic nuclei (AGN). However, in comparing the X-ray and 24 μm detections, only one cluster galaxy (in RX J0152) is detected in both and rejected. While the AGN fraction in clusters seems to increase with redshift (Eastman et al. 2007), the estimated AGN fraction is only 2% at $z \sim 0.6$. Johnson et al. (2003) also find evidence that at $z \sim 0.8$, any excess X-ray AGN are located at $R > 1$ Mpc, whereas we focus on the central Mpc of each cluster. Although we cannot completely rule out possible contamination by weak obscured AGN, we have excluded X-ray AGN and thus assume that the galaxies detected by MIPS are powered by dusty star formation; see Marcillac et al. (2007) for a more detailed argument on why this is a reasonable assumption.

3. RESULTS

3.1. *Color-Magnitude Diagrams*

Figure 1 presents the color-magnitude diagrams of the five main clusters with photometry from H07. Because the MIPS sensitivity varies from cluster to cluster, we apply a SF rate limit of 5 $M_\odot$ yr^{-1}. The first immediate observation is that the number

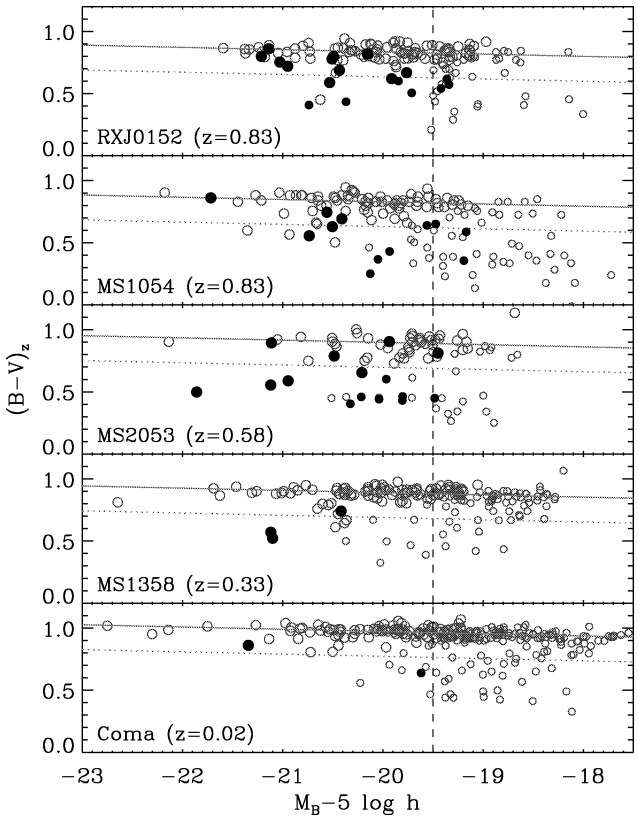

FIG. 1.—Rest-frame color-magnitude diagrams for spectroscopically confirmed members in the main cluster sample. Filled red circles are MIPS detections with SF rates $\geq 5\ M_{\odot}\ \mathrm{yr}^{-1}$ (where all clusters are better than 50% complete). The larger symbols represent galaxies with $\log_{10}(M_*) \geq 10.6$. The rest-frame B-band magnitude has been corrected for passive luminosity evolution, as determined from the fundamental plane (van Dokkum et al. 1998a). The vertical dashed line is the rest-frame B-band magnitude selection limit of -19.5. The solid diagonal line is the best fit to the red sequence galaxies, adopting the slope of van Dokkum et al. (1998b), and the dotted line denotes $\Delta(B - V) = -0.2$ mag; only galaxies below the dotted line would be part of the standard BO sample. [*See the electronic edition of the Journal for a color version of this figure.*]

of strongly star-forming galaxies increases significantly with redshift. Using a field galaxy sample drawn from the same photometric and spectroscopic catalogs, we estimate a possible field contamination at $z = 0.83$ to be ~8% (i.e., no more than one galaxy per cluster). In Figure 1, the dotted lines represent the original color criterion for BO galaxies. The ratio of the number of cluster galaxies with MIR SF rate $\geq 5\ M_{\odot}\ \mathrm{yr}^{-1}$ above this color cut to the number of blue galaxies [$\Delta(B - V) < -0.2$] increases with redshift.

3.2. *The Mid-Infrared Butcher-Oemler Effect*

For each cluster, we compute and plot in Figure 2 the fraction of confirmed star-forming cluster members after selecting by rest-frame B-band magnitude ($M_B \leq -19.5$), clustercentric distance,[6] and MIR SF rate ($\geq 5\ M_{\odot}\ \mathrm{yr}^{-1}$). The errors on $f_{\mathrm{SF,MIPS}}$ represent the range that can be produced by taking the minimum and maximum conversion factors from $F_{24\ \mu\mathrm{m}}$ to $F_{8-1000\ \mu\mathrm{m}}$ instead of a single average value for each cluster and by varying the different selection thresholds by amounts comparable to the errors on each of these parameters.

Figure 2 shows that the fraction of galaxies in clusters with

[6] While the optical observations generally extend to $R_P > 1.5$ Mpc, the MIPS imaging for MS 1358 only extends to ~1 Mpc (~50%–60% of $r200$ for these clusters).

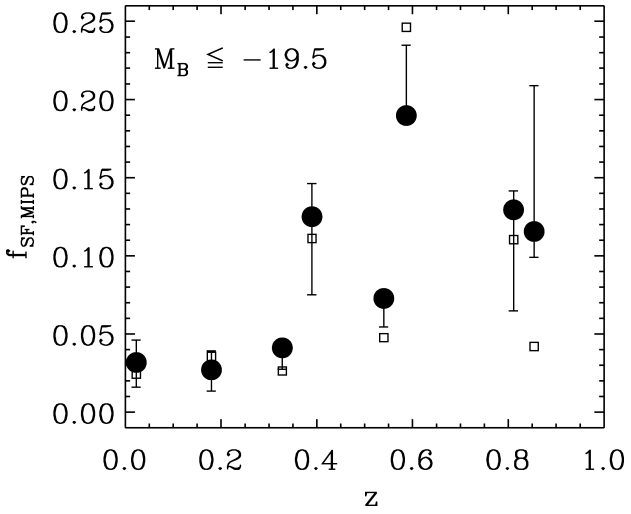

FIG. 2.—Fraction of confirmed cluster galaxies that are star forming as revealed by the MIPS 24 μm observations. Only considered are members with MIR SF rates $\geq 5\ M_{\odot}\ \mathrm{yr}^{-1}$ that are brighter than $M_B = -19.5$ and located within 1 Mpc of the cluster centers (*filled circles*) and 500 kpc (*open squares*). The points for the two $z \sim 0.83$ clusters are offset slightly in z for clarity.

MIR SF rates $\geq 5\ M_{\odot}\ \mathrm{yr}^{-1}$ steadily climbs from ~3% locally to ~13% at $z = 0.83$. Because H07 showed that a cluster's morphological composition can vary depending on whether members are selected by mass or by luminosity, we apply an additional stellar mass cut of $\log_{10}(M_*) \geq 10.6$ (Fig. 3). The mass cut is applied only to the five main clusters for which uniform photometry and thus stellar masses are available; the remaining three clusters are shown only as upper limits. While the mass cut attenuates the increase in fraction of star-forming members, it does not completely suppress the trend. Thus, the MIR BO effect is not due to an increase in the fraction of faint, low-mass members temporarily brightened by strong star formation.

4. DISCUSSION

Having established an increase in the fraction of MIR-detected galaxies from $z \sim 0$ to $z \sim 0.8$, we stress that optical studies are likely underestimating the increase in star-forming

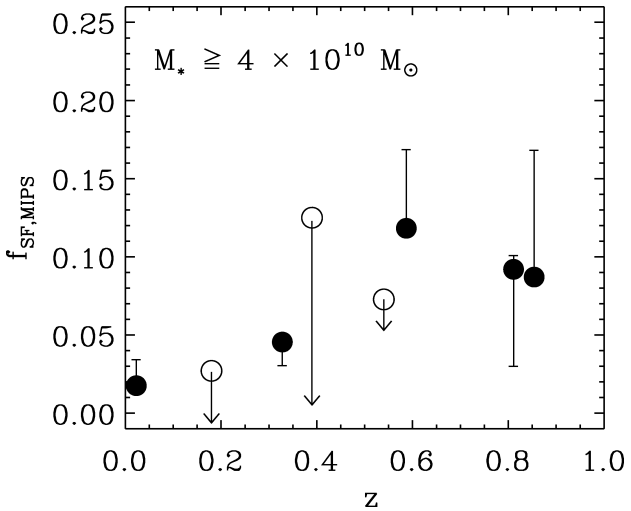

FIG. 3.—As in Fig. 2, the fraction of confirmed star-forming cluster galaxies (MIR SF rate $\geq 5\ M_{\odot}\ \mathrm{yr}^{-1}$, $M_B \leq -19.5$, $R_P < 1$ Mpc), but now with the additional stellar mass cutoff of $\log_{10}(M_*) \geq 10.6$ for the five main clusters (*filled circles*). Stellar masses are not available for the remaining three clusters; they are shown as upper limits (*open circles*).

cluster galaxies with redshift. As seen in Figure 1, an increasing number of strong dust-obscured star-forming members appear on or near the red sequence at higher redshifts; these are not included in traditional color-selected BO studies. The late-type morphologies of these members support our intepretation of dusty star formation and red colors due to extinction (see also A901/902; Wolf et al. 2005).

Using the standard BO definition of $\Delta(B-V) < -0.2$, the fraction of blue galaxies with $M_B \leq -19.5$ and $R_P < 1$ Mpc at $z \sim 0.8$ is ∼11%; however, including the red, massive, star-forming members raises the total fraction of blue/star-forming members to ∼23%. We note that for the five main clusters, the increase in the blue/star-forming fraction due to these red, star-forming members is {1.1, 1.2, 1.3, 1.7} at $z = \{0.02, 0.33, 0.59, 0.83\}$; i.e., the relative importance of including red, dusty star-forming members increases with redshift.

Is this increase linked to galaxy infall? In Figure 2, both CL 0024 ($z \sim 0.4$) and MS 2053 ($z \sim 0.6$) are above the general trend established by the other six clusters. Both CL 0024 and MS 2053 have enhanced star formation compared to other clusters at similar redshift, and both have bimodal redshift distributions. CL 0024 is made of two colliding subclusters (Czoske et al. 2002) and has an unusually large number of luminous infrared galaxies (Coia et al. 2005). Similarly, Tran et al. (2005) conclude that MS 2053 has a significant number (>25%) of infalling galaxies; these members tend to be blue and star forming. Both CL 0024 and MS 2053 are accreting a large number of new members and have high fractions of dusty star-forming galaxies. We speculate that the increase in star-forming members reflects the recent accretion of new members, i.e., galaxy infall, and that such events are more frequent at higher redshift due to the process of cluster assembly (Ellingson et al. 2001; Tran et al. 2005; Loh et al. 2008). As further evidence of this, 80% of the MIPS-detected galaxies in the $z \sim 0.8$ clusters are more than 700 kpc from the cluster cores in projected distance, and thus the MIR Butcher-Oemler effect is significantly altered by considering only the inner 500 kpc of the clusters (open symbols in Fig. 2).

5. SUMMARY

We present the first comprehensive study of *SST*/MIPS 24 μm observations for eight massive, X-ray–luminous galaxy clusters spanning a wide redshift range ($0.02 < z < 0.83$). Uniform photometry, high-resolution *HST* imaging, and extensive redshift catalogs enable us to measure the fraction of members with strong, dust-obscured star formation. The fraction of cluster galaxies with MIR star formation rates $\geq 5\,M_\odot$ yr^{-1} increases from 3% in Coma to ∼13% in clusters at $z = 0.83$, and this trend is evident in both luminosity-selected ($M_B \leq -19.5$) and mass-selected ($M_* \geq 4 \times 10^{10} M_\odot$) samples.

Optically based studies increasingly underestimate the total amount of star formation in cluster galaxies with redshift because many of these dusty red star-forming members are missed in color-selected samples. These tend to be late-type galaxies that are red because of dust extinction which disguises their high levels of obscured star formation (>5 $M_\odot$ yr^{-1}). Defining the SF fraction to include both optically blue and red, but MIPS-detected, members doubles the fraction at $z = 0.83$ from ∼11% to ∼23% ($R_P < 1$ Mpc).

Finally, our study indicates that the BO effect and the increase in obscured star-forming members are linked to galaxy infall: 80% of the MIR-detected members at $z \sim 0.8$ are outside the cluster cores ($R_P > 0.7$ Mpc), and the two clusters at $z < 0.8$ that are accreting a substantial number of new members also have an enhanced fraction of galaxies with MIR SF rates $\geq 5\ M_\odot$ yr^{-1}.

We are grateful to C. Papovich and L. Bai for advice on MIPS data reduction and to G. Rudnick for useful discussions. A. S. and K. T. acknowledge support from the Swiss National Science Foundation (grant PP002-110576).

Facilities: HST (WFPC2, ACS), Spitzer (MIPS).

REFERENCES

Bai, L., et al. 2007, ApJ, 664, 181
Balogh, M. L., Schade, D., Morris, S. L., Yee, H. K. C., Carlberg, R. G., & Ellingson, E. 1998, ApJ, 504, L75
Bardeau, S., et al. 2007, A&A, 470, 449
Beijersbergen, M. 2003, Ph.D. thesis, Rijksuniversiteit Groningen
Bell, E. F. 2002, ApJ, 577, 150
Blakeslee, J. P., et al. 2006, ApJ, 644, 30
Butcher, H., & Oemler, A., Jr. 1978, ApJ, 219, 18
———. 1984, ApJ, 285, 426
Caldwell, N., & Rose, J. A. 1997, AJ, 113, 492
Cardiel, N., Elbaz, D., Schiavon, R. P., Willmer, C. N. A., Koo, D. C., Phillips, A. C., & Gallego, J. 2003, ApJ, 584, 76
Coia, D., et al. 2005, A&A, 431, 433
Couch, W. J., Ellis, R. S., Sharples, R. M., & Smail, I. 1994, ApJ, 430, 121
Couch, W. J., & Sharples, R. M. 1987, MNRAS, 229, 423
Czoske, O., Moore, B., Kneib, J.-P., & Soucail, G. 2002, A&A, 386, 31
Dale, D. A., & Helou, G. 2002, ApJ, 576, 159
Dale, D. A., et al. 2007, ApJ, 655, 863
Demarco, R., et al. 2005, A&A, 432, 381
Donahue, M., Voit, G. M., Scharf, C. A., Gioia, I. M., Mullis, C. R., Hughes, J. P., & Stocke, J. T. 1999, ApJ, 527, 525
Dressler, A., & Gunn, J. E. 1982, ApJ, 263, 533
Dressler, A., Oemler, A. J., Butcher, H. R., & Gunn, J. E. 1994, ApJ, 430, 107
Duc, P.-A., et al. 2002, A&A, 382, 60
Eastman, J., Martini, P., Sivakoff, G., Kelson, D. D., Mulchaey, J. S., & Tran, K.-V. 2007, ApJ, 664, L9
Ellingson, E., Lin, H., Yee, H. K. C., & Carlberg, R. G. 2001, ApJ, 547, 609
Fisher, D., Fabricant, D., Franx, M., & van Dokkum, P. 1998, ApJ, 498, 195
Geach, J. E., et al. 2006, ApJ, 649, 661
Holden, B. P., et al. 2007, ApJ, 670, 190 (H07)
Houck, J. R., et al. 2005, ApJ, 622, L105
Johnson, O., Best, P. N., & Almaini, O. 2003, MNRAS, 343, 924
Kauffmann, G. 1995, MNRAS, 274, 153
Kennicutt, R. C., Jr. 1998, ARA&A, 36, 189
Lavery, R. J., & Henry, J. P.1988, ApJ, 330, 596
Lavery, R. J., Pierce, M. J., & McClure, R. D. 1992, AJ, 104, 2067
Loh, Y., Ellingson, E., Yee, H. K. C., Gilbank, D. G., Gladders, M. D., & Barrientos, L. F. 2008, ApJ, 680, 214
Makovoz, D., & Khan, I. 2005, in ASP Conf. Ser. 347, Astronomical Data Analysis Software and Systems XIV, ed. P. Shopbell, M. Britton, & R. Ebert (San Francisco: ASP), 81
Makovoz, D., & Marleau, F. R. 2005, PASP, 117, 1113
Marcillac, D., Rigby, J. R., Rieke, G. H., & Kelly, D. M. 2007, ApJ, 654, 825
Mathieu, R. D., & Spinrad, H. 1981, ApJ, 251, 485
Moran, S. M., Ellis, R. S., Treu, T., Smail, I., Dressler, A., Coil, A. L., & Smith, G. P. 2005, ApJ, 634, 977
Moran, S. M., Ellis, R. S., Treu, T., Smith, G. P., Rich, R. M., & Smail, I. 2007, ApJ, 671, 1503
Oemler, A. J., Dressler, A., & Butcher, H. R. 1997, ApJ, 474, 561
Poggianti, B. M., et al. 2006, ApJ, 642, 188
Tran, K.-V. H., van Dokkum, P., Illingworth, G. D., Kelson, D., Gonzalez, A., & Franx, M. 2005, ApJ, 619, 134
Tran, K.-V. H., et al. 2007, ApJ, 661, 750
van Dokkum, P. G., Franx, M., Kelson, D. D., & Illingworth, G. D. 1998a, ApJ, 504, L17
van Dokkum, P. G., Franx, M., Kelson, D. D., Illingworth, G. D., Fisher, D., & Fabricant, D. 1998b, ApJ, 500, 714
Wolf, C., Gray, M. E., & Meisenheimer, K. 2005, A&A, 443, 435
Zhang, Y.-Y., Böhringer, H., Mellier, Y., Soucail, G., & Forman, W. 2005, A&A, 429, 85